staining were assessed by immunohistochemistry. (Table 1) The results of molecular profile and clinical outcome were compared between the 2 types.
Results: KRAS mutation was identified in 17% of IPMN-Os and in 58% of IPMN-PBs. BRAF mutation was identified only in one IPMN-O. Loss of SMAD4, overexpression of p53 and nuclear ß-catenin expression were also found in a fraction of both types (IPMN-PB ≥ IPMN-O) (Table 1).

Table 1

	IPMN-PB	IPMN-O
KRAS	7(58%)*	3(17%)*
BRAF	0	1(6%)
PIK3CA	0	0
SMAD4[a]	4(33%)	2(12%)
TP53[b]	7(58%)**	1(6%)**
β-catenin[c]	2(17%)	3(17%)

a: any loss of nuclear expression, b: presence of expression in > 30% of tumor cells, c: any nuclear expression, *: p<0.05, **: p<0.01.

92% of IPMN-PB and 50% of IPMN-O contained invasive adenocarcinoma. At the end of follow-up (1 to 165 months after resection), 4 patients with IPMN-PB and 2 with IPMN-O died of the disease. All showed invasive carcinoma. Although the overall survival was better in IPMN-O than in IPMN-PB (Kaplan-Meier survival analysis, $p < 0.05$), there was no difference in survival of cases with invasive components between the 2 types ($p = 0.16$).
Conclusions: The results of our study indicate that molecular alterations as well as biological behavior are not significantly different between IPMN-O and IPMN-PB, especially in those with invasive components. In addition, it is the first report demonstrating KRAS mutation in IPMN-O, thus supporting the notion that IPMN-O is not distinct from the other types of IPMN.

1668 Arginase-1, a New Immunohistochemical Marker of Hepatocytes and Hepatocellular Neoplasms

BC Yan, C Gong, J Hart. University of Chicago Medical Center, Chicago, IL.
Background: The distinction of hepatocellular carcinomas (HCCs) from metastatic tumors to the liver often presents a diagnostic challenge that carries significant impact on subsequent prognostication and therapeutic management. The number of immunohistochemical markers for pathologic identification of hepatocytes remains limited to HepPar-1, polyclonal CEA and CD10, with alpha-fetoprotein and glypican-3 labeling HCCs. The HepPar-1 antigen was recently shown to correspond to the urea cycle enzyme carbamoyl phosphate synthetase [Butler SL, Dong H, Cardona D, Jia M, Zheng R, Zhu H, Crawford JM and Liu C. (2008) Lab. Invest. 88: 78-88]. Previous immunohistochemical studies have established that arginase-1 (ARG1), another enzyme involved in the urea cycle, is also expressed in normal human liver with a high degree of specificity [Multhaupt H, Fritz P and Schumacher K. (1987) Histochemistry 87: 465-470].
Design: We examined the expression of ARG1 in 24 HCCs, 15 macroregenerative nodules (MRNs), 3 dysplastic nodules (DNs), 4 intrahepatic cholangiocarcinomas, 23 breast carcinomas, 15 pulmonary adenocarcinomas, 15 prostate carcinomas, 99 colonic adenocarcinomas and 111 salivary gland tumors by immunohistochemistry using a commercially available antibody (Sigma Aldrich) and heat retrieval methods for antigen unmasking to determine its viability as a hepatocellular marker.
Results: We found that ARG1 demonstrated strong, diffuse, nuclear and cytoplasmic expression in both normal hepatocytes and hepatocellular neoplasms: 23 of 24 HCCs (95%) exhibited strong, diffuse immunoreactivity for ARG1. All examined MRNs and DNs showed similar reactivity. In contrast, biliary epithelium, endothelial cells and Kupffer cells were non-reactive. A single combined HCC-cholangiocarcinoma exhibited ARG1 positivity only in the HCC component. In addition, one prostatic adenocarcinoma was also reactive. All other tumors examined were non-reactive.
Conclusions: ARG1 appears to be a specific marker of hepatocytes and, as such, can be used to distinguish hepatocellular carcinomas from metastatic tumors in the liver. The identification of ARG1 as a specific immunohistochemical marker of hepatocytes may lead to its development as a useful diagnostic adjunct in routine surgical pathology practice.

1669 The Effect of Tumor Heterogeneity on the Prognostic Value of Ki67 Labeling Index in Well-Differentiated Neuroendocrine Tumors (NETs) Metastatic to the Liver

Z Yang, LH Tang, DS Klimstra. Memorial Sloan-Kettering Cancer Center, New York, NY.
Background: The Ki67 labeling index correlates with survival in patients with NETs. A proposed grading scheme classifies well-differentiated NETs into two categories based on Ki67 index: low grade (<3%), and intermediate grade (3-20%). Metastatic NETs to the liver are often diagnosed by random needle core biopsy, and the Ki67 index is thus determined on this limited sample. The reliability of the Ki67 index has been questioned based on possible intratumoral heterogeneity.
Design: Forty-three resected cases of NET metastatic to the liver were collected. Triplet tissue cores from three random sites in the paraffin blocks were used to construct a tissue microarray, representing simulated biopsies. Immunohistochemical staining for Ki-67 was performed, and the labeling index was determined by image analysis. The overall Ki67 index was determined for each core triplet, and heterogeneity was defined as the presence of grade discordance among the 3 samples. The mitotic count of the original slides was also determined: low grade <2/10 HPF, and intermediate grade 2-20/10 HPF.
Results: Thirty-four cases had a low Ki67 index, while 8 cases had an intermediate Ki67 index; these included one case that showed an intermediate Ki67 index in one block and low in another. By Kaplan-Meier survival analysis, intermediate overall Ki67 index predicted worse overall, disease-free, and progression-free survival ($p<0.005$), compared to a low Ki67 index. Intermediate mitotic activity predicted worse progression-free survival ($p<0.05$), but not overall and disease-free survival. Thirty-eight cases (83%) were considered homogenous for Ki67 index (34 low grade and 4 intermediate grade) on simulated random biopsy, and 8 cases (17%) had heterogeneity. Statistically, there were significantly more overall intermediate grade cases showing Ki67 heterogeneity (Fisher's exact test, $p=0.02$), and in those cases, the Ki67 indices were close to the 3% cutoff value (range 2.1-3.6%). One of three cases also showed significant Ki67 heterogeneity between different metastatic foci.
Conclusions: By imaging analysis, Ki67 labeling index has significant prognostic value for patients with NETs metastatic to the liver. In most cases in particular the low grade ones, random sampling has no clear effect on the prognostic value of the Ki67 index. Ki67 staining of core biopsies usually provides an adequately reliable method of proliferation assessment for prognosis.

Neuropathology

1670 Distinction between Complete and Partial 1P/19Q Losses in Gliomas: A Novel User-Friendly Approach

A Ariza, C Carrato, MD Lopez, M Domingo-Sabat, MT Lopez, K Beyer. Hospital Germans Trias i Pujol, Autonomous University of Barcelona, Badalona, Barcelona, Spain.
Background: Complete loss of both 1p and 19q has been associated with oligodendrogliomas, whereas partial 1p loss has been related to aggressive astrocytomas. However, the two most frequently used methods for 1p and/or 19q loss determination (fluorescent in situ hybridization and microsatellite amplification) focus on 1p34-36 and 19q13 only and are thus unable to accurately distinguish between complete and partial arm losses.
Design: In an attempt to discriminate between the types of arm loss, we used semiquantitative real-time PCR of telomeric and centromeric sequences on 1 p (SPAG17, ATG4), 19q (DPY19L3, RPS9), 1q (PYGO2 and GREM2), and 19p (COPE, FUT3) in a series of 69 astrocytomas and 10 oligodendrogliomas. The deltadeltaCt method was used for relative quantification of PCR products. Conventional LOH study of 1p and 19q by microsatellite amplification was also performed in all cases.
Results: Among astrocytomas, of the 11 instances showing 1p loss and the 12 instances showing 19q loss by microsatellite amplification, our approach demonstrated the loss to be complete for 1p in just 1 instance and for 19q in just 4 instances. In contrast, each of the 10 oligodendrogliomas, all showing both 1p and 19q loss by microsatellite amplification, revealed both complete 1p and complete 19q loss by our method.
Conclusions: The rapid and easy-to-use approach herein described is a useful complementary tool for accurately determinating whether chromosome losses are complete or partial in gliomas. Of practical interest, it abolishes the need for patient's normal tissue or peripheral blood as control.

1671 Atypical Mycobacterial Brain Abscess Presenting as Spindle Cell Lesion in an Immunocompetent Patient

K Arkun, DA Gordon, C Lincoln, M Levi, J Bello, CE Keller, KM Weidenheim. Montefiore Medical Center, Bronx, NY; Albert Einstein College of Medicine, Bronx, NY.
Background: Mycobacterium Avium Complex (MAC) organisms are important secondary infections in immunocompromised patients and are usually seen in patients with AIDS. Disseminated and focal MAC infections usually involve the lungs, gastrointestinal tract and peripheral lymph nodes. It is unusual to see involvement of the central nervous system, where MAC produces imaging findings similar to tuberculoma.
Design: We present a 52-year-old HIV-negative man with a previous history of non-caseating pulmonary granulomata and lung carcinoma treated with radiotherapy, who presented with 6 month history of slowly progressive dizziness, headache,and gait disturbance with frequent falls. Tissue obtained at subtotal resection was cultured and paraffin sections were examined with the light microscope.
Results: Neuroimaging revealed a large, complex, multiloculated, ring-enhancing cystic lesion centered in the left tentorium with extension into supratentorial and infratentorial compartments. Compression of the fourth ventricle resulted in hydrocephalus that required subtotal resection of the mass and aspiration of caseous yellow material. The specimen consisted of a variably cellular proliferation of CD68-positive spindle cells arranged in bands, fascicles and ill-defined nodules. A few lymphocytes and plasma cells were seen, and a single giant cell was present. Delicate rod-shaped organisms were faintly positive using methenamine silver, Brown-Brenn Gram staining and Ziehl-Neelsen staining. The bacilli were strongly positive with Fite and Kinyoun staining, and DNA probes confirmed their identification as MAC. M. tuberculosis was not present on DNA analysis.
Conclusions: This MAC brain abscess presented as a complex mass with differential diagnosis that includes infections and tumor. Its exuberant spindle cell proliferation had a pseudosarcomatous appearance and produced difficulty in diagnosis because granulomatous features were found only focally. Clinical correlation and culture results were critical in obtaining the correct diagnosis. In the appropriate clinical setting, infectious processes including MAC-related brain abscess, should be ruled out before making the diagnosis of a spindle cell neoplasm.

1672 Expression of SALL-4 Distinguishes Intracranial Germ Cell Neoplasms from Other Central Nervous System Tumors

JK Deisch, D Rakheja, P Shang, CL Hladik, CL White, J Raisanen. University of Texas Southwestern Medical Center, Dallas, TX; Children's Medical Center, Dallas, TX.
Background: Germ cell neoplasms are relatively uncommon intracranial tumors accounting for 0.3-0.6% of primary intracranial neoplasms in the Western hemisphere and 2-3% in Eastern Asia. Most occur in children and young adults, most in males, and

most in the midline in the sellar or pineal regions. Despite the characteristic localization, diagnosis of an intracranial germ cell neoplasm may be difficult.
Design: We used immunohistochemistry to assess expression of the stem cell transcription factor SALL-4 in 30 germ cell neoplasms that occurred intracranially and 75 other central nervous system tumors including 69 neoplasms and 6 inflammatory lesions. We examined expression in 19 intracranial germinomas, 4 mature teratomas, 2 immature teratomas, 3 choriocarcinomas, and 1 embryonal carcinoma and 16 glioblastomas, 4 pilocytic astrocytomas, 5 ependymomas, 5 choroid plexus papillomas, 6 medulloblastomas, 1 rhabdoid tumor, 5 pituitary adenomas, 5 craniopharyngiomas, 7 pineal parenchymal neoplasms, 5 meningiomas, 5 primary central nervous system (CNS) lymphomas, 5 metastatic carcinomas, 2 cases of intracranial sarcoidosis, 1 of Langerhans cell histiocytosis, and 3 other nonspecific inflammatory lesions, 1 of the pituitary and 2 of the cavernous sinus.
Results: There was strong nuclear expression of SALL-4 by the neoplastic cells of all germinomas and choriocarcinomas, and the embryonal carcinoma. No cells of the mature teratoma expressed SALL-4, but there was weak nuclear expression by neuroectodermal cells in 1 of 2 immature teratomas. There was also weak nuclear expression by cells of 1 CNS rhabdoid tumor. No cells of any other primary CNS neoplasm expressed SALL-4, nor was there expression by cells of the metastatic neoplasms or any of the inflammatory lesions.
Conclusions: The findings indicate that SALL-4 is expressed by cells of primitive intracranial germ cell neoplasms but, with the possible exception of rhabdoid tumors, not other CNS neoplasms or inflammatory lesions. Immunohistochemistry to detect nuclear expression of SALL-4 may be useful in the diagnosis of intracranial germ cell neoplasms.

1673 Developmentally Arrested Structural Elements (DASEs) Preceding CNS Tumorigenesis in VHL Disease

EA Falke, SB Shively, J Li, RR Lonser, AO Vortmeyer. Yale School of Medicine, New Haven, CT; National Institute of Neurological Disorders and Stroke, Bethesda, MD; George Washington University, Washington, DC.
Background: Previously we demonstrated developmentally arrested structural elements (DASEs) composed of hemangioblast progenitor cells in the peripheral nervous system of VHL patients. A small subset of DASEs may progress to frank tumor, hemangioblastoma (HB). Central nervous system (CNS) tumors in VHL disease, however, are most frequently observed in the cerebellum, suggesting a site of origin in CNS, from unknown cells and unknown topographic sites. We performed a structural and topographic analysis of cerebellar tissues from VHL patients to identify and characterize DASEs in the CNS.
Design: To search for DASEs, we examined the entire cerebella of 5 patients with VHL disease and 3 non-VHL disease controls. A total of 599 blocks were processed from the 8 cerebella. A hematoxylin-eosin (HE) stained section for each block was screened for DASEs at high power. Whenever DASEs were detected histologically, the respective paraffin block containing DASE material and the block coronally en face to it were serially sectioned at 6 microns. Immunohistochemical (IHC) labeling for CD34, CD31, CAIX, brachyury, HIF1, and HIF2 was performed on unstained sections from DASE containing blocks.
Results: 10 cerebellar DASEs were detected in the 385 blocks of VHL cerebella. No DASEs were seen in 214 blocks from the cerebella of 3 controls. DASES preferentially involve the molecular layer of the dorsal cerebellum. DASEs are composed of poorly differentiated cells that express CAIX and HIF2, but not HIF1. In contrast, HB tumor cells are IHC positive for HIF2 and HIF1, as well as CAIX.Consistent with their immature phenotype, DASEs rarely or never expressed brachyury, while HB cells were immunopositive for brachyury.
Conclusions: Prior studies have shown that peripheral nervous system hemangioblastomas are preceded by developmentally arrested structural elements (DASEs). For the first time, we identify similar (DASEs) in the CNS of VHL patients. DASEs in cerebellum are composed of developmentally arrested hemangioblast progenitor cells in the molecular layer, with activation of HIF2 but not HIF1. In contrast, frank tumors acquire a hemangioblastic phenotype with additional activation of HIF1 and expression of brachyury, among other markers of hemangioblastic differentiation.

1674 Heat Shock Protein (HSP) Expression in Diffuse Gliomas: A Potential Therapeutic Target

A Gonzalez, R Kolhe, S Sharma. Medical College of Georgia, Augusta, GA.
Background: HSPs are molecular chaperones which facilitate tumor growth and resistance to radiation/chemotherapy. HSP90 antagonists are being pursued in therapeutic trials. Scant data is available in diffuse gliomas (DG). We evaluated the expression of HSP27, 70 and 90 in DGs.
Design: Representative paraffin blocks from 17 diffuse gliomas: 5 astrocytomas grade-II (A), 5 anaplastic astrocytomas (AA), 3 glioblastomas (GBM), 1 glioblastoma-oligodendroglioma type (GBM-O), and 3 oligodendroglioma grade-II (OG), were immunostained with antibodies to HSP27, 70 and 90. Percentage positivity of neoplastic cells was evaluated (less than 10% considered negative). Expression of HSPs was validated on endometrium and internal vascular controls.
Results: The immunoreactivity was cytoplasmic. The percentage of positive cases is tabulated. Among astrocytic tumors, HSP27 expression was more pronounced in GBM, and in larger/pleomorphic or gemistocytic cells in all 3 grades. In contrast, HSP70 and HSP90 showed positivity mainly in small/intermediate sized neoplastic cells. In GBM, 2 cases showed peri-necrotic and 1 perivascular accentuation. Hyperplastic vessels were highlighted in 1 GBM. Among oligodendroglial tumors, HSP 70 and 90 were positive in 2 and 1 cases respectively, whereas HSP27 was reciprocally positive in GBM-O and one grade II OG with increased Ki67 labeling. The mean value of HSP27 percentage positivity of tumor cells was higher in high-grade as compared to low-grade diffuse gliomas, most pronounced in GBM as well as GBM-O (see table).

HSP Stain Distribution in High-grade diffuse gliomas

Tumor Type	HSP27 + cases	Mean % positive tumor cells	HSP70 + cases	Mean % positive tumor cells	HSP90 + cases	Mean % positive tumor cells
AA (5)	3	32	5	52	5	57
GBM (3)	3	58	3	65	3	45
GBM-O (1)	1	90	0	0	0	0
Total = 9	7 (77%)	60	8 (88%)	39	8 (88%)	34

HSP Stain Distribution in Low-grade diffuse gliomas

Tumor Type	HSP27 + cases	Mean % positive tumor cells	HSP70 + cases	Mean % positive tumor cells	HSP90 + cases	Mean % positive tumor cells
A (5)	3	36	5	60	5	52
OG (3)	1	8	2	36	1	20
Total = 8	4 (50%)	22	7 (87%)	48	6 (75%)	36

Conclusions: HSP27, 70 and 90 are expressed in diffuse gliomas. HSP27 showed increased expression in GBM, in larger/gemistocytic cells, and among low-grade astrocytic compared to oligodendroglial tumors. This expression pattern of HSPs suggests their role in the growth of diffuse gliomas, and as potential therapeutic targets in high-grade gliomas.

1675 Loss of Heterozigosity on 10q23 (PTEN Region) Is a Relevant Predictor of Survival in High Grade Astrocytomas

MA Idoate, J Echeveste, R Diez Valle, MD Lozano, B Bejarano. University of Navarra, Pamplona, Navarra, Spain.
Background: PTEN is a suppressor gene located in the chromosome region 10q23.3 which is considered a genetic marker of glioblastomas. Loss of heterozigosity (LOH) around PTEN could be a relevant prognostic marker in high-grade astrocytomas, but a systematic study with a number of microsatellites is not available. We have realized a study of LOH of 10q23 in a large series of patients diagnosed of high-grade astrocytoma with a complete follow-up.
Design: Fifty-nine patients were operated and diagnosed as glioblastomas (43) and anaplastic astrocytomas (16) between 1994 and 2003. The mean age of these patients was 47 y.o. (6-78) and the mean of Karnofsky was 81%. All patients received the same protocol treatment. Twelve cases of diffuse grade II were also included as a reference, A LOH PCR analysis by using 4 microsatellites of 10q23.3 chromosome (D10S579, -S2491, -S541AF, -Ma086wg9) on frozen tumors was applied. LOH evaluation was made by two observers and the non-clear cases were studied by a semi-quantitative method according to international standard references. A statistical study was applied.
Results: Tumors with LOH deletion showed no distinctive histological features respect to those without deletions. A frequent LOH on 10q23,3 PTEN region was observed in 25%, 35% and 40% of grade III and in 23%, 46% and 31% of grade IV, tumors, according to 1, 2 or ≥3 deleted loci respectively. In grade II astrocytomas, no deletion was observed. In glioblastomas, the mean of overall survival after diagnosis was significant according to the number of deleted loci (905 days for no deleted loci against 205 days for patients with ≥3 deleted loci). A striking correlation between LOH deletion (≥ 1 locus deleted) around PTEN and overall survival was observed in both grade IV (Log-Rank, Mantel-Cox, p= 0.01) and grade III (Log-Rank, Mantel-Cox, p= 0.03) astrocytomas.
Conclusions: According to our results, LOH deletion on 10q23 is a strong marker of survival in high-grade astrocytomas, and it is not associated to distinctive tumor histological features.

1676 Comparative Study of the Nestin Expression in the Invasive Border of Glioblastoma and in Reactive Glial Tissue

MA Idoate, R Diez Valle, J Echeveste, MD Lozano, T Labiano, A Panizo. University of Navarra, Pamplona, Navarra, Spain.
Background: We have previously shown that surgery done with 5-ala fluorescence allows highly precise separate sampling of the invasive border of the tumor in glioblastoma (GBM). Nestin is a type VI intermediate filament considered as a marker for tumor stem cell and could be used in the identification of peripheral glioblastoma cells. However, an ample characterisation of this marker in different pathological contexts is not available. To study the value of nestin, invasive cells in the periphery of glioblastoma were compared with the reactive glia in both active and chronic gliosis.
Design: In 32 consecutive patients the fluorescent quality of the tissue was used to take biopsies from the tumor center, from the border and from the surrounding normal-looking tissue. This group was compared with the reactive glia in 30 biopsies from patients with brain metastasis, vascular malformations and mesial temporal gliosis in chronic epilepsy. All samples were analysed by immunostaining against nestin and GFAP.
Results: In all GBM cases, central tumor areas and pathological vessels stained strongly with nestin. The density of nestin expression decreased gradually around the tumor, but in all cases strong nestin expression was also seen in the vessels walls and in many different cells in the peritumor areas. Some of these cells looked like typical astrocytes while many others had one or two wide processes or no process at all. In metastases and vascular malformations active gliosis around also showed intense expression of nestin with cell phenotype similar to the GBM border. However, in mesial (chronic) gliosis, nestin expression in the glia was absolutely negative. Glia GFAP expression was similar in the periphery of GBM and in the other series.
Conclusions: Nestin is a glial acute reaction marker, not a specific tumor stem cell marker, as strong nestin expression accompanies glioblastoma as well as acute glial reaction. However, in the chronic mature glia, no expression of nestin is observed at all.

1677 Oligodendroglial Tumors with Desmoplasia: A Case Series

ME Jentoft, C Giannini, S Rossi, R Mota, BL Hoesley, RB Jenkins, FJ Rodriguez. Mayo Clinic College of Medicine, Rochester, MN; Regional Hospital, Treviso, Italy.

Background: Oligodendroglial tumors may show a variety of morphologic patterns; however examples of these tumors with desmoplasia are rare and not completely characterized.

Design: Among the in house and consultation practice we encountered 5 unusual oligodendroglial tumors due to the presence of marked desmoplasia. We reviewed the clinical data and the histologic findings including immunohistochemical and cytochemical stains. Immunohistomemistry was scored on a 4 tiered scale (0-3). FISH studies for 1p19q and t(1;19) were performed.

Results: Patients included 3 males and 2 females, mean age at time of primary surgery was 48 years (range 31-57). Four (of 5) patients are alive, mean follow-up 4.4 years from initial diagnosis (range 1.25 -11.3). All 5 patients had tumor recurrence or progression, mean 4.1 years (range 1.1 to 10.6): 3 had a subtotal resection; 1 had a gross total resection; and in 1 case extent of tumor resection was not known. One patient died of disease 1.9 years from the date of initial surgery. Two tumors were described as firm/tough in texture and consistence at the time of surgery. Tumors were classified as anaplastic oligoastrocytomas (3) or oligodendrogliomas (2), all WHO grade III. Characteristic morphologic features included tumor nests/nodules with surrounding fibrosis/ desmoplasia (n=4), and cords/single cell infiltration (n=1), minigemistocytes (n=3), endothelial hypertrophy (n=4), and necrosis in 1 case. Mean mitotic index was 7 mitoses per 10 HPF (400X). Immunohistochemical studies demonstrated immunoreactivity for GFAP (n=5/5), synaptophysin with a paranuclear "dot" like pattern (n=3/5), PDGFRα 2-3+ (n=5/5), PDGFRβ 3+ (n=3/3), and EGFR 1-2+ (n=3/4). p53 protein expression was 1-2+ (n=5/5) and MIB-1 labeling index was moderate (n=5/5). Four (of 5) tumors demonstrated 1p19q co-deletion and the remaining tumor, an oligoastrocytoma, 1p deletion with intact 19q. t(1:19) was identified in 2 (of 3) cases tested, both also with 1p19q co-deletion, the t(1;19) negative case being the one with 1p loss only.

Conclusions: Oligodendroglial tumors with prominent desmoplasia are rare. They appear to incite a desmoplastic response when in proximity of the leptomeninges. Oligodendroglial tumors with desmoplasia in our series were all anaplastic (WHO grade III). As expected, with oligodendroglial tumors, the majority of cases demonstrate 1p19q co-deletion.

1678 c-Myc Protein Expression Is Prognostic of Survival in Embryonal Brain Tumor Patients

DAR Kanagasabapathy, Y Morales-Odia, CG Eberhart. Johns Hopkins University, Baltimore, MD.

Background: Medulloblastoma and other embryonal neoplasms represent the most common childhood brain tumors. Despite significant advances in their treatment, a high proportion of surviving patients suffer from long-term debilitating neurologic side effects. This is in part due to a lack of reliable prognostic markers in routine histopathologic examination which might allow lesser doses of craniospinal irradiation to be given to patients whose tumors have a less aggressive profile. c-myc mRNA levels and gene dosage have been shown previously to be associated with anaplasia and poor patient outcomes in medulloblastoma, however, c-myc protein expression has not been examined. The goal of our study is therefore to evaluate c-Myc protein as a potential prognostic marker using formalin-fixed, paraffin embedded samples.

Design: We studied c-myc expression in 80 patients whose embryonal tumors were included on a tissue microarray. Immunohistochemistry was performed with a newly developed rabbit monoclonal antibody from Epitomics (Burlingame, CA, Clone Y69) using standard techniques. Cores were scored in a semi-quantitative fashion (0 to 3+) for nuclear expression of antigen. At least two intact cores were required for a case to be included in the analysis.

Results: The 65 cases that could be evaluated included 54 cases of medulloblastoma, 8 cases of supratentorial primitive neuroectodermal tumor (sPNET) and 3 atyptical teratoid/rhabdoid tumors. Of these 23% (15/65) showed nuclear immunopositivity for c-Myc while the remainder (77%) were negative. Five cases were 2+ positive, three cases showed 3+ positivity and the remainder was 1+ in staining intensity. c-Myc positive cases were present in all categories and cytoplasmic immunoreactivity was limited to only a few tumors. Cases stratified on the basis of expression of c-Myc protein (positive vs negative) showed a significant difference in survival rates by logrank analysis of Kaplan-Meier curves (p=0.03).

Conclusions: Our data suggest that c-Myc protein immunoreactivity may represent a novel predictor of shorter survival in patients with embryonal brain tumors.

1679 Id4 Expression in Diffuse Gliomas: Is There a Correlation with Lineage and Grade?

R Kolhe, A Gonzalez, S Sharma. MCG, Augusta.

Background: Id4 (inhibitor of differentiation), a member of helix-loop-helix (HLH) transcription factor family, dimerizes with basic HLH factors such as Olig1 and Olig2, to prevent transcriptional induction of downstream target genes. In neural progenitor cells, Id4 induction by BMP-4 treatment was noted to allow OLIG1/2 to co-localize with cytoplasmic Id4, thereby inhibiting oligodendroglial differentiation. Enforced expression of Id4 stimulates proliferation & blocks differentiation of oligodendrocyte precursor cells. Also, increased Id4 levels (mRNA/Protein) were detected in GBM & glioma cell lines**.** Therefore, we studied the immunoexpression of ID4 in diffuse gliomas (DG) of different lineages & grades.

Design: Immunostaining with antibody to ID4 was retrospectively examined on representative paraffin sections from 17 DG: these included 5 astrocytomas WHO grade-II (A), 5 anaplastic astrocytomas (AA), 3 glioblastomas (GBM), 1 glioblastoma-oligodendroglioma type (GBM-O), & 3 oligodendroglioma grade-II (OG). Percentage positivity of neoplastic cells for both nuclear & cytoplasmic staining was evaluated (<10% considered negative).

Results: Both nuclear & cytoplasmic immunoreactivity was noted. The percentage of positive cases is tabulated. Almost all DG (95%) showed nuclear immunoreactivity (except one recurrent post-radiation A) spread across all lineages and grades. In contrast, cytoplasmic ID4 expression was restricted to a proportion of high-grade astrocytic tumors, mainly gemistocytic/larger tumor cells. Oligodendroglial tumors, including GBM-O showed no significant cytoplasmic staining.

Id4 Stain Distribution in High-grade DG

Tumor Type	Nuclear ID4 + cases	Mean % positive tumor cells (Range)	Cytoplasmic ID4 + cases	Mean % positive t umor cells (Range)
AA (5)	5	47 (25-80)	3 (gemistocytic)	42 (0-80)
GBM (3)	3	68 (50-80)	2	17 (0-25)
GBM-O (1)	1	85	0	0
T= 9	9 (100%)	58 (25-85)	5 (55%)	29 (0-80)

Id4 Stain Distribution in Low-grade DG

Tumor Type	Nuclear ID4 + cases	Mean % positive tumor cells (Range)	Cytoplasmic ID4 + cases	Mean % positive tumor cells (Range)
A (5)	4	38 (5-80)	0	7 (1-9)
OG (3)	3	37 (20-50)	0	6 (1-9)
T= 8	7 (88%)	38 (5-80)	0	7 (1-9)

Conclusions: Nuclear ID4 expression was noted in 95% DG of all lineages & grades. The restricted immunoexpression of significant cytoplasmic Id4 only to a proportion of high-grade astrocytic tumors (in contrast to oligodendroglial tumors) suggests its selective role in transformation of astrocytic (especially gemistocytic) tumors, & may have prognostic value.

1680 Assessment of O(6)-Methylguanine-DNA Methyltransferase (MGMT) Promotor Methylation and Protein Expression in Pituitary Adenomas

SH Lee, YS Ko, MJ Lee, TS Hwang, WS Kim, HS Han, SD Lim. Konkuk University School of Medicine, Seoul, Republic of Korea; Konkuk University Medical Center, Seoul, Republic of Korea.

Background: Many studies have demonstrated the value of assessment of O(6)-methylguanine-DNA methyltransferase (MGMT) level of various cancers in predicting the response of patients to therapy with alkylating agents. Recently, temozolomide therapy has been suggested to be a clear therapeutic benefit for the treatment of resistant or aggressive pituitary adenomas (PAs). The aim of this study was to investigate quantitative methylation status of O(6)-methylguanine-DNA methyltransferase (MGMT) promoter gene and its protein expression in PAs.

Design: A total of 34 consecutive PAs were selected from the archives of the department of pathology of Konkuk University Medical Center from 2005 to 2009. Clinicopathologic data including hormonal status and imaging findings were obtained from medical records. Quantitative methylation data at 13 CpG sites of MGMT promotor gene were obtained by pyrosequencing and MGMT protein expression was evaluated in tissue microarry by immunohistochemistry.

Results: The cases included non-functional PAs (n=21), prolactinomas (n=5), both prolactinoma and growth homrome PAs (n=1), growth hormone PAs (n=4), gonado troph adenoma (n=1), and adrenocorticotropic PAs (n=2). The recurrent PAs and clinically invasive PAs are 7 and 10 cases, respectively. The average methylation frequency of MGMT promotor gene of all cases was 15.4% ranging from 7.1% to 25.7%. 7 PAs showed completely negative immunoreactivity (IR) and 13 PAs revealed very weak IR in the tumor cells. 6 PAs showed diffuse and strong nuclear and cytoplasmic IR. The remaining PAs revealed the heterogeneous IR with less than 30% of nuclear stainability. There are no correlations between MGMT promotor methylation and its protein expression or clinical parameters.

Conclusions: These results suggest that MGMT promoter methylation and protein loss are a frequent event in PAs, and hence Temozolomide therapy can be considered to a new adjuvant therapeutic modality in PAs.

1681 Carbonic Anhydrase IX (CA9) Is a Reliable Marker for Hemangioblastoma

M Li, J Song, P Pytel. Univ. of Chicago, Chicago, IL.

Background: Hemangioblastomas (HAB) are either sporadic (75%) or associated with von Hippel-Lindau (VHL) syndrome (25%). The stromal cells of HAB are believed to be neoplastic, although their lineage of differentiation remains unresolved. Morphologically, HAB can mimic other intracranial tumors such as certain types of meningioma and hemangiopericytoma (HPC). Diagnostic markers for HAB are lacking, although a recent study reported D2-40 as a potential marker. Many sporadic HAB have detectable VHL mutations that lead to activation of the HIF-VEGF pathway. CA9 is a downstream protein of this pathway, and has been shown to be a reliable marker for clear cell renal cell carcinoma (CCRCC), another tumor associated with VHL syndrome. This study investigated the expression patterns of CA9, VEGF and D2-40 in HAB, HPC and meningioma.

Design: With IRB approval, 24 HAB (3 associated with VHL syndrome), 5 meningiomas and 5 HPC were selected from University of Chicago pathology archive. Immunostains for CA9, VEGF, and D2-40 were performed. The staining extent was recorded as the percentage of positive tumor cells, and classified as: diffuse (>80%), focal (1-80%), and negative. Staining intensity (strong, moderate or weak) and subcellular localization were also recorded.

Results: All except one HAB showed diffuse, strong, membranous CA9 staining in the tumor cells, similar to the pattern seen in CCRCC. Meningiomas and HPC only had focal, weak to moderate, cytoplasmic CA9 staining mostly limited to peri-necrotic areas, which is a well known non-specific pattern caused by focal hypoxia. VEGF staining was more diffuse in HAB than in meningiomas and HPC ($p < 0.01$, Mann-Whitney U test); and its intensity varied from weak to moderate.

Cases	CA9			VEGF		
	Diffuse	Focal	Negative	Diffuse	Focal	Negative
HAB	23	1	0	21	3	0
Meningioma	0	5 *	0	1	4	0
HPC	0	5 *	0	1	4	0

* Mostly limited to peri-necrotic areas.

In contrary to a previous report, D2-40 staining was variable in HAB (1 diffuse, 14 focal, 9 negative). It was positive in meningiomas (4 diffuse, 1 focal), and negative in HPC. There was no difference between sporadic and VHL associated HAB cases for all markers.

Conclusions: CA9 and VEGF were consistently expressed in HAB, supporting a role for the HIF-VEGF pathway in the tumorigenesis of sporadic and syndromic HAB. CA9 showed a distinct diffuse, strong, membranous staining pattern in almost all HAB cases, making it a reliable marker for HAB in the differential diagnosis of intracranial tumors.

1682 Angiocentric Glioma: A Clinicopathologic Review of Five Tumors with Identification of Associated Cortical Dysplasia

TB Marburger, RA Prayson. Cleveland Clinic Foundation, Cleveland, OH.

Background: Angiocentric glioma is a rare, epilepsy-associated, low grade neoplasm with a characteristic perivascular growth pattern which has been recently codified in the 2007 WHO classification of CNS tumors. The purpose of this study is to describe the clinicopathologic features of five angiocentric gliomas and to evaluate for coexistent malformation of cortical development (MCD)/cortical dysplasia.

Design: Retrospective review of the clinicopathologic features of 5 angiocentric gliomas (3 females and 2 males; median age at surgery 10 yrs, range 3-19 yrs). Adjacent MCD was classified according to criteria outlined by Palmini et al.

Results: Seizures were the most common presenting symptom (n=4); one patient presented with headaches. Four of the tumors were located in the parieto-occipital, parietal, and temporal cortex and one case arose in the thalamus. All tumors consisted of an angiocentric growth pattern of bipolar spindle cells with mild pleomorphism. Three tumors also demonstrated a focal solid growth pattern. Two cases exhibited a population of cells with rounded nuclei resembling oligodendroglial cells. Evidence of adjacent MCD (focal cortical dysplasia) was observed in 3/4 cases with sufficient tissue for evaluation; all were Palmini et al Type I lesions (Type IA n=2; Type IB n=1). Calcifications (n=2) and microcystic elements (n=1) were observed in a minority of cases. Mitotic activity, necrosis, vascular proliferation, and meningeal extension were not observed. Ki-67 labeling indices were <4% in all cases. Ultrastructural evaluation (n=4) exhibited evidence of ependymal differentiation in one case. All patients are living (median follow-up 3 years postoperatively, range <1-10 years). No tumor recurrence following gross total resection (n=3) has been reported. Post-surgical follow up revealed near complete cessation of seizure symptoms (Engel Class 1) for 3/3 patients who underwent gross total resection and only mild improvement in seizure symptoms (Engel Class 4) in the single case with subtotal resection.

Conclusions: The thalamic location of one tumor represents an undescribed location for this typically superficial cortical tumor. Rare cases may exhibit a population of cells resembling oligodendroglial cells. A subset of angiocentric gliomas, similar to other low grade chronic epilepsy-related tumors of childhood, may be associated with coexistent MCD, suggesting a developmental basis to their origin.

1683 High Incidence of *BCL-6* Gene Abnormalities in Primary Central Nervous System Diffuse Large B-Cell Lymphoma in Immunocompetent Patients

SE Martin, EM Hattab, MA Al-Abbadi, RA Stohler, GH Vance, M Czader. Indiana University School of Medicine, Indianapolis, IN; James H. Quillen Veterans Affairs Medical Center, Mountain Home, TN.

Background: Primary central nervous system diffuse large B-cell lymphomas (PCNSL) are rare neoplasms characterized by a dismal prognosis. Despite emerging consensus that they arise from lymphoid cells at the post-germinal center stage of differentiation, the majority of the cases of PCNSL are positive for BCL-6, a marker selectively expressed by germinal center B cells. B-cell-6 is a proto-oncogene that codes for a zinc finger transcription repressor required for germinal center formation and function. We have studied the incidence of *BCL-6* gene rearrangements in a well characterized group of PCNSL.

Design: Twenty-two cases of PCNSL were studied. Immunostains for CD10, BCL-6 and MUM-1 were used to determine germinal center vs. post-germinal center cell origin. In-situ hybridization for EBER was performed in each case. Fluorescence in-situ hybridization was performed in formalin fixed, paraffin embedded tissue using breakapart probe for *BCL-6*, and dual color/dual fusion probes for *MYC/IGH* and *IGH/BCL2*. Survival was calculated using a Kaplan-Meier method.

Results: Thirteen patients were female. Median age at diagnosis was 64 years (range 13-80). None of the patients had history of immunodeficiency. Eighteen cases were of post-germinal center cell phenotype. BCL-6 immunostain was positive in 20 cases. One case was positive for EBER. Eight cases (36%) showed rearrangements of *BCL-6* gene. Additional three cases showed numerical abnormalities of *BCL-6* (2 monosomy and 1 trisomy). The remaining 11 cases had normal *BCL-6* signal. The majority of cases with *BCL-6* rearrangement lacked *MYC/IGH* and *IGH/BCL2* translocations with only one case being positive for *IgH/BCL2* fusion. Two cases with rearranged *BCL-6* showed trisomy/tetrasomy of *BCL-2* gene, and one showed evidence of genomic instability with trisomy/tetrasomy for all studied probes. Even though there was a trend for shorter survival in patients with *BCL-6* gene rearrangements, Kaplan-Meier analysis did not reach statistical significance.

Conclusions: High incidence of abnormalities of the *BCL-6* gene was detected by FISH analysis in PCNSL in immunocompetent individuals. The majority of cases were of post-germinal center cell origin and were EBV negative.

1684 Clincopathologic and Immunohistochemical Characteristics of Metastatic Breast Carcinoma to the Brain: A Neurosurgical Series of 59 Cases

SE Martin, KA Johnson, P Steeg, EM Hattab. Indiana University School of Medicine, Indianapolis, IN; National Cancer Institute, Bethesda, MD.

Background: Metastatic breast cancer to the central nervous system (CNS) is second only to lung in frequency. Affected patients typically have advanced systemic disease by the time CNS involvement is manifested. Patients with triple negative primary breast cancer and those with Her2 amplification usually are at an increased risk for metastasis. Currently, therapeutic options are limited with surgery generally offered to those with solitary lesions, and prognosis is poor (20% one-year survival). Therefore, greater understanding of this disease and its risk factors is essential for improved clinical outcome.

Design: Fifty-nine cases of metastatic breast cancer to the CNS were identified. Two cohorts were created: one for which paraffin blocks from both the primary and the metastatic lesions were available (matched) and another for which only the metastasis was available (unmatched). Cases were evaluated for various demographic, clinical and pathologic parameters. Immunohistochemistry for ER, PR, Her2 and EGFR, and Her2 FISH analysis were performed. Survival data was assessed.

Results: Patients were overwhelmingly Caucasian (87%). The median age at diagnosis of the CNS metastasis was 56 years with an average latency of 32 months. Most metastases were supratentorial (60%). The vast majority of tumors were infiltrating ductal type with a high SBR score. 44% were triple negative, while 19% were ER/PR negative, but Her2 positive. Sixteen patients were assigned to the matched cohort, of which 11 (69%) maintained an identical immunoprofile. Intense EGFR immunoreactivity was observed in a minority of cases and seemed to correlate with triple negative hormonal status. Follow-up interval ranged from 3 to 567 months, with a median follow-up of 57 months. At last follow-up, 25% of patients were still alive. The median overall survival from the time of diagnosis of CNS metastasis was 14 months.

Conclusions: The majority of solitary breast cancer metastases to the CNS were supratentorial, of the infiltrating ductal type, and either triple negative or ER/PR negative-Her2 positive. In at least two-thirds of the cases, the immunoprofile of the metastatic lesion was predictive of that of the primary tumor. Loss of ER or PR expression occurred in the remaining cases. In general, patients experienced poor clinical outcome; however, multivariate analysis of various clinical, pathologic and immunohistochemical characteristics is underway.

1685 Novel Translocation t(9;17)(q32;q24) in a Glioneuronal Tumor

RD McComb, LA Bruch, CA Reyes, MJ Puccioni, JA Bridge. University of Nebraska Medical Center, Omaha, NE; University of Iowa, Iowa City, IA; Children's National Medical Center, Washington, DC; Midwest Neurosurgery, Omaha, NE.

Background: Glioneuronal tumors (GNT) with mixed neurocytic/ganglioid and glial components are rare and difficult to subclassify. One recently recognized variant, papillary GNT, is identified by the presence of a specific pseudopapillary architecture. Genetic data on such tumors are limited; gain of structurally aberrant chromosome 7 material was identified in an isolated case of papillary GNT.

Design: A seven-year-old boy underwent gross total resection of a large parieto-occipital cystic tumor that showed irregular contrast-enhancement. In addition to histologic and immunohistochemical evaluation, a representative portion of the tumor was examined by conventional cytogenetic analysis using standard procedures. The karyotypes were described according to the International System for Human Cytogenetic Nomenclature (ISCN 2009).

Results: Pathologic evaluation revealed a mixed glioneuronal tumor with a prominent synaptophysin-positive neurocytic/ganglioid cell component intimately mixed with a GFAP-positive glial element. Much of the tumor exhibited sheet-like growth with a delicate microvasculature. Focal areas showed a pseudopapillary architecture in which hyalinized blood vessels were ensheathed by a layer of tumor cells. GFAP-positive cells were located in the diffuse and interpapillary areas as well as perivascular regions. Mitoses were not identified, and the Ki67 immunolabeling index was low. Cytogenetic analysis revealed a diploid clone characterized by the following reciprocal translocation as the sole anomaly: t(9;17)(q32;q24). Six cells with a normal male 46,XY complement were also observed.

Conclusions: This tumor showed features of a papillary GNT with a prominent glial component. A novel 9;17 translocation was identified as the sole karyotypic abnormality, suggesting it could play an important role in the pathogenesis of this tumor and potentially serve as a useful diagnostic marker if it proves to be recurrent. In addition, these findings focus attention on specific regions of chromosomes 9 and 17 that may contain genes central to the glioneuronal neoplastic process.

1686 Composite Ganglioglioma/Dysembryoplastic Neuroepithelial Tumor: A Clinicopathologic Study of 6 Cases

KM Napekoski, RA Prayson. Cleveland Clinic Foundation, Cleveland, OH.

Background: Ganglioglioma (GG) and dysembryoplastic neuroepithelial tumor (DNT) are both low grade glioneuronal neoplasms that most commonly occur in the temporal lobe in association with chronic epilepsy. Rare case reports of tumors with composite features of GG and DNT have been reported.

Design: We retrospectively reviewed the clinicopathologic features of 6 composite GG/DNT tumors (5 females and 1 male; median age at time of surgery 18 years, age range 5-37 years).

Results: All 6 patients had medically intractable epilepsy, tumors in the temporal lobe, and were treated with subtotal resection. Four patients are currently seizure free (postoperative followup intervals: 88, 91, 108, and 140 months); one patient had decreased seizures (postoperative followup interval of 177 months); and one was lost to follow up. Histologically, all of the tumors were multinodular. Half contained two types of histologically distinct nodules: some nodules had features consistent with

typical microcystic DNT (range of 15-75% of the tumor) and some demonstrated features consistent with typical GG (range of 10-85% of the tumor). Three tumors contained nodules which demonstrated a hybrid of oligodendroglial type cells mixed with atypical astrocytes and normal appearing neurons. Four tumors demonstrated areas of multinodular GG. Three out of four evaluable tumors demonstrated adjacent malformation of cortical development/cortical dysplasia (Palmini type Ia). None of the tumors contained mitotic activity, vascular proliferation, or necrosis. Two tumors demonstrated focal meningeal extension. Ki-67 immunostaining was performed on 4 of the tumors with indices <1% in all cases.
Conclusions: Composite GG/DNT tumors commonly arise in the temporal lobe in young patients with chronic epilepsy. Histologically, these multinodular tumors appear to maintain distinct areas with features of GG and DNT in addition to foci where the two patterns are merged. A subset of composite GG/DNT tumors appear to be associated with adjacent malformation of cortical development.

1687 Atypical Teratoid Rhabdoid Tumors in Adults: Report of Six Cases with Molecular Cytogenetics Analysis

L Neder, MR Ericson-Johnson, X Wang, A Tay, AM Oliveira, BW Scheithauer. Mayo Clinic, Rochester, MN.
Background: Atypical Teratoid Rhabdoid Tumors (AT/RTs) are rare malignant embryonal tumors of the CNS most commonly found in young infancy and early childhood. Loss of INI1 protein expression is seen in almost all AT/RTs, and most tumors exhibit loss or mutations of the *INI1* gene *(hSNF5/SMARCB1)* located on chromosome 22q11.2. AT/RT only rarely affects adults; isolated cases have been reported but none with molecular analysis. Herein, we report the clinicopathologic and molecular signature of six cases of adult AT/RTs.
Design: All six AR/RT specimens were obtained from the consultation files of one of us (BWS) or were operated at Mayo Clinic between 1998 and 2009. Immunohistochemistry analysis for *INI1* expression was performed in all instances. Interphase molecular cytogenetic analysis was performed using a customer designed fluorescence in situ hybridization (FISH) probe spanning the *SMARCB1/INI1* locus paired with a reference probe spanning the *BCR* locus. All analyses were done on 4µm paraffin-embedded sections according to a standardized protocol. Ten typical infantile AT/RT were used as positive controls, and three CNS PNETs and 1 normal cerebral cortex served as negative controls.
Results: The patients (five female, one male) were age 23 to 44 years (mean age, 32 ± 3 SD). Of the six tumors, three involved the cerebrum (frontal and temporal lobes) and three the pineal region. Histologically, they were composed variably of rhabdoid cells, epithelioid cells in ribbons and cords, and mesenchymal appearing spindle cells in a basophilic matrix. No tumors exhibited a PNET component. Molecular cytogenetic studies demonstrated deletions of the *INI1* locus in four tumors: 2 homozygous and 2 heterozygous deletions. One tumor showed a molecular cytogenetic signature consistent with rearrangement of chromosome 22 between the *INI1* and *BCR* loci, and the other a normal *INI1* molecular cytogenetic signature.
Conclusions: Adult AT/RTs differ somewhat from those of childhood with respect to female predominance, supratentorial location, and morphology (absence PNET component). Our preliminary molecular cytogenetic data suggest that adult AT/RT shows similar mechanisms of *INI1* inactivation when compared to their typical infantile form.
Spport: CAPES (Proc. No. 1429-08/6) and Mayo Fundation.

1688 Injection Site Pseudosarcomas in Piriformis Syndrome

DC Phan, X Fan, OTM Chan, E Himmelfarb, SI Bannykh. Cedar-Sinai Medical Center, Los Angeles, CA.
Background: Treatment for patients with refractory nerve entrapment and piriformis syndromes often includes localized injection of anesthetic and/or corticosteroids. The histologic appearances of these injection sites have not been well-described. We have recently seen three cases in which the exuberant reactive fibroblastic/myofibroblastic proliferation at these injections sites mimicked a sarcoma. As the clinical history provided on pathology requisition forms is frequently incomplete, the lesions may easily be misinterpreted as neoplastic.
Design: 266 cases with muscle resection for piriformis syndrome were evaluated. Three cases including, 2 males and 1 female aged 36, 44 and 59, respectively showed exuberant reactive fibroblastic/myofibroblastic proliferation. All had received local injections of corticosteroids and/or anesthetics. As the patients continued to have pain, partial resection of the piriformis muscle was subsequently performed for nerve release.
Results: The histologic findings in all 3 cases were similar and included: a florid, highly cellular, cytologically atypical and mitotically active spindle cell proliferation diffusely infiltrating between skeletal myofibers and associated with myonecrosis/phagocytosis, degenerating and regenerating myofibers and a mixed inflammatory infiltrates. In the most striking index case the MIB-1 labeling index was >80%. Immunohistochemically, the proliferating cells were of three categories: 1) MyoD1+/desmin+/SMA+ skeletal myocytes, MyoD1-/Desmin-/SMA-/caldesmon+ myofibroblasts and 3) quadruple negative presumed fibroblasts. No staining of the lesional cells for CD31 and S100. Features arguing against a neoplastic process were the gross and clinical absence of a mass lesion and the pattern of diffuse infiltration between skeletal muscle fibers. However, the reparative etiology of the lesions was confirmed only after investigation of the clinical history. Confirmatory, in one of the cases the affected muscle was re-excised with findings of unremarkable muscle with a possible fibrosis.
Conclusions: Misinterpretation of a florid reactive process as a sarcoma is one of the leading causes of medical malpractice lawsuits in the field of soft tissue pathology (nodular fasciitis being the most commonly cited example). We herein report another clinical scenario in which this pitfall may be encountered.

1689 Microscopic Thrombi in Anaplastic Astrocytoma (AA) Predicts Worse Survival

NF Prayson, P Koch, L Angelov, RA Prayson. University School, Hunting Valley, OH; CCLCM, Cleveland, OH; Cleveland Clinic, Cleveland, OH.
Background: It is well-known that certain brain tumors, such as glioblastoma, have a high incidence of intratumoral thrombi and an increased risk of developing deep venous thrombosis (DVT). The previously reported incidence of intratumoral thrombosis in AA is relatively low. The purpose of this study is to determine whether AA patients (pts) with intratumoral vascular thrombi have a worse survival than AA pts without thrombi.
Design: Retrospective review of 101 patients (pts) (60 males, 41 females; age range 1-85 years (yrs), mean 53.3 yrs) with AA (WHO grade III). Thrombi were counted (number of thrombi/blood vessels evaluated/10 high power fields) in the initially resected tumor (69 biopsies, 32 subtotal resections) and correlated with a variety of parameters including survival and development of postoperative DVT.
Results: Intravascular thrombi were identified in 17 AA (17%) (9 biopsies, 8 subtotal resections), of tumors with thrombi, the percentage of blood vessels with thrombi ranged from 1.5-20% (mean 5.6%). Ten pts were known to have received chemotherapy and 16 pts radiotherapy. Sixteen of 17 pts died of tumor (mean survival 15.4 months (mos), range 1-45 mos) and one patient was alive with tumor at 180 mos. The remaining 84 AA (83%) (60 biopsies, 24 subtotal resections) had no intravascular tumor thrombi; 57 pts received chemotherapy and 67 pts received radiotherapy. After follow-up, 75 of 84 pts without thrombi died of tumor (mean survival 26.5 months, range 0.5 - 139 months), 4 pts were alive (7, 8, 42, and 77 mos) and 5 pts were lost to follow-up. Evidence of DVT was found by ultrasound in 2 of 11 (18.2%) AA pts with thrombi who were tested versus 10 of 54 (18.5%)AA pts without thrombi.
Conclusions: Microscopic intratumoral thrombi were identified in 17% of AA. Pts with thrombi had a worse survival (mean 15.4 mos) versus AA pts without intratumoral thrombi (mean 26.5 mos), although the difference did not reach statistical significance. There appears to be no correlation between the presence or absence of intratumoral thrombi and the development of DVT.

1690 Tumors Arising in the Setting of Pediatric Chronic Epilepsy

RA Prayson, J Fong, I Najm. Cleveland Clinic Foundation, Cleveland, OH.
Background: Along with malformations of cortical development (MCD), hippocampal sclerosis, and remote ischemic damage, tumors are among the more common identifiable causes of medically intractable seizures in pediatric age patients. This study reviews one institution's 20 year experience with tumors arising in this clinical setting.
Design: Retrospective review of 129 pediatric patients (less than 18 years of age, 65 females (54%)) with tumors and medically intractable seizures encountered during a 20 year period of time (1989 - 2009). Using the most recent WHO classification of brain tumors, tumor type and grade were assessed.
Results: The most common sites of origin included temporal lobe (N=77, 59.7%), parietal lobe (N=20, 15.5%), and frontal lobe (N=15, 11.6%). WHO grade included 73 (56.6%) grade I tumors, 32 (24.8%) grade II tumors, and 18 (14%) grade I/II tumors. In 6 cases (4.7%), a WHO grade is not associated with mass. Tumor types included : ganglioglioma (N=48, 37.2%), dysembryoplastic neuroepithelial tumor (N=17, 13.2%), low grade astrocytoma (N=15, 11.6%), low grade mixed glioma (N=8, 6.2%), low grade oligodendroglioma (N=5, 3.9%), meningioangiomatosis (N=4, 3.1%), angiocentric glioma (N=3, 2.3%), and dysembryoplastic neuroepithelial tumor/ganglioglioma composite tumor (N=3, 2.3%). Less frequently observed lesions (N=1 or 2) included pilocytic astrocytoma, protoplasmic astrocytoma, pleomorphic xanthoastrocytoma, and glioneuronal hamartoma. In 18 cases, distinction between low grade glioma and low grade glioneuronal tumor could not be definitively made. Coexisting MCD was noted in 19.4% of cases. In 4 tumors, coexistent hippocampal sclerosis was identified. Ki-67 labeling indices were less than 5% in all (N=51) cases assessed. Of 25 tumors evaluated for chromosome 1p status, only one low grade mixed glioma demonstrated evidence of deletion; only 1/22 evaluated tumors (a low grade mixed glioma) showed evidence of chromosome 19q deletion.
Conclusions: Collectively, WHO grade I glioneuronal tumors account for slightly more than half of all neoplasms which cause intractable epilepsy in pediatric patients. A significant minority of tumors (N=18, 14%) were difficult to definitively classify as glioma versus glioneuronal tumor, due on extent of sampling. Coexistent pathologies including MCD and hippocampal sclerosis may be observed in a significant minority of tumors, suggesting a possible developmental origin to some tumors arising in this setting.

1691 Dual Pathology in Chronic Epilepsy Patients with Neoplasms

RA Prayson. Cleveland Clinic Foundation, Cleveland, OH.
Background: Neoplasms are a well established cause of medically intractable or chronic epilepsy. Certain tumors, including gangliogliomas (GG) and dysembryoplastic neuroepithelial tumors (DNT), are well known to be associated with cortical dysplasia. This study retrospectively examines the incidence of dual pathology in patients with tumors and chronic epilepsy.
Design: Retrospective view of 270 tumors arising in patients with medically intractable epilepsy encountered during a 20 year period (1989 to 2009). Dual pathology was noted in 50/270 (17.8%) patients, including 27 males (54%) with a mean age at surgery of 17.7 years (range 1-52 years).
Results: The vast majority of lesions n=40 (80%) were located in the temporal lobe and less commonly parietal lobe (n=4) and occipital lobe (n=3). Tumor diagnoses included GG (n=29), DNT (n=10), low grade glial/glioneuronal neoplasm (n=5), low grade astrocytoma (n=2), angiocentric glioma (n=1), low grade mixed glioma (n=1), DNT/GG mixed tumor (n=1), and meningioangiomatosis (n=1). Forty-one (82%) tumors represented WHO grade I neoplasms. Concomitant pathology included malformation of

cortical development (cortical dysplasia) in 40 patients (80%) (Palmini et al type I: n=37; Palmini et al type II: n=3). Hamartias were identified in 10 patients (20%), hippocampal sclerosis in 4 patients (8%), and nodular heterotopia in 1 patient (2%).
Conclusions: Dual pathology was observed in a significant subset of chronic epilepsy patients with neoplasm (17.8% in this study). Most tumors were WHO grade I neoplasms and represented GG or DNET. The true incidence of dual pathology was likely underrepresented, given the limited extent of adjacent nontumoral tissue sampling in cases of resected tumor. Coexistent pathology may account for the incidence of recurrent or residual epilepsy in patients who undergo tumor resection.

1692 Utility of Autopsy in Uncovering Unexpected Neuropathology

RA Prayson. Cleveland Clinic Foundation, Cleveland, OH.
Background: Autopsy rates have significantly declined in the last several decades for a variety reasons. One often cited reason is that with the improvement of various diagnostic modalities including imaging, diagnoses are more commonly and accurately made premortem, obviating the need for an autopsy. The purpose of this study is to compare neuropathologic (NP) findings from recent autopsies with findings from autopsies performed in the early 1980s to assess whether there is a decrease in the incidence of unexpected findings.
Design: Respective review of 328 autopsy brains from 1984-1985 (200 males, 61.0%; mean age 56.3 years) compared with 289 autopsy brains from 2007-2008 (160 males, 55.4%; mean age 57.6 years). The incidence of unexpected NP diagnoses, and in particular, unexpected diagnoses which were determined to be the major cause of death, were documented and compared.
Results: Unsuspected NP diagnoses were found at autopsy in 139 (42.4%) of cases from 1984-1985 versus 112 (38.8%) of cases from 2007-2008. The neuropathology was felt to significantly contribute to the cause of death in 72 patients (22.0%) in 1984-1985 versus 57 patients (19.7%) in 2007-2008. The most common cause of unexpected NP diagnoses in 1984-1985 included: acute/subacute infarct (14.8%), remote infarct (13.2%), hemorrhage (10.6%), metastatic cancer (4.2%) and vascular malformations (4.2%). The most common unexpected NP diagnoses in the 2007-2008 cohort included acute/subacute infarct (27.7%), Alzheimer's disease (22.3%), hemorrhage (18%), remote infarct (17.0%) and meningitis (9.8%). The incidence of unexpected NP diagnoses being the main cause of death was 5.2% in 1984-1985 versus 3.1% in 2007-2008.
Conclusions: Despite differences between styles of the autopsy report, pathologists, and types of cases autopsied, the findings would suggest that suspected NP findings are still found in over one-third of autopsy cases. Autopsy NP examination still plays a role in uncovering unexpected diagnoses which may be responsible for the main cause of death in a small but significant percentage of causes, underscoring the continued utility of brain and spinal cord examination at autopsy.

1693 Expression of Microglial Markers in Diffuse Large B-Cell Lymphomas of the Central Nervous System

A Sasaki, H Yamaguchi, M Ikeda, A Yokohama, Y Nakazato, M Shimizu. Saitama Medical University, International Medical Center, Hidaka, Saitama, Japan; Gunma University School of Health Science, Maebashi, Gunma, Japan; Gunma University Graduate School of Medicine, Maebashi, Gunma, Japan.
Background: Diffuse large B-cell lymphomas (DLBCL) are the most common type of primary central nervous system lymphoma (PCNSL). Our previous study indicated that the number of apoptotic cells were significantly higher in CNS DLBCL than in non-CNS DLBCL. The great majority of tumors that have been previously termed as microglioma actually represent PCNSL. In this study, we examined CNS DLBCL, non-CNS DLBCL and a human B cell lymphoma cell line to determine the relationship between microglia and lymphoma cells.
Design: Twenty cases of CNS DLBCL and 11 cases of non-CNS DLBCL were studied by immunohistochemistry (IHC) using antibodies against glucose transporter 5 (GLUT5), Iba1 and CD68 (PG-M1). Both double-labeling with terminal deoxynucleotidyl transferase-mediated dUTP-nick end labeling (TUNEL) and Iba1 IHC and double immunofluorescence analysis of GLUT5 and CD20 (L26) were performed in a representative case of CNS DLBCL. GLUT5 immunostaining in neoplastic cells of DLBCLs was semiquantitatively evaluated by counting the percentage of labeled cells. Immunocytochemical and Western blot analyses of GLUT5 expression were performed using the Raji cell line.
Results: In all cases of CNS-DLBCLs, activated microglia and macrophages were labeled with all three antibodies against GLUT5, Iba1 and CD68. Double labeling of TUNEL and Iba1 IHC showed some macrophages with phagocytosis of apoptotic cells. In all cases of CNS DLBCL, neoplastic lymphocytes were stained with GLUT5 antibody in a variable number in all cases, but not stained with either Iba1 or CD68 antibodies. Semi-quantitatively, five of 20 cases (25%) showed numerous GLUT5-positive lymphoma cells (more than 50% labeled cells). In double immunofluorescence staining for GLUT5 and L26, double-positive cells were observed. In non-CNS DLBCLs, lymphoma cells were stained with GLUT5, but not with Iba1 or CD68. The GLUT5 immunoreactivity was observed on Raji cells by both immunocytochemistry and Western blot analysis.
Conclusions: The present study indicated that CNS DLBCLs contain a large number of microglia and macrophages and that macrophages could be involved in the removal of apoptotic cells. Our findings demonstrated that expression of GLUT5 is frequently induced on lymphoma cells in the CNS, although this GLUT5 expression on lymphoma cells is unlikely to support the microglial origin of CNS lymphoma.

1694 Metastatic Carcinomas Presenting as Dural-Based Masses Mimicking Primary Intracranial Neoplasia

NM Savage, CH Alleyne, R Figueroa, S Sharma. Medical College of Georgia, Augusta, GA.
Background: Clinical presentation with dural-based metastasis mimicking meningiomas is rare and described mostly as case reports from diverse primary locations. Proposed pathways include vascular spread and direct extension from calvarial or brain metastases.
Design: We retrospectively reviewed 6 cases with resection of dural-based metastatic carcinomas; five were clinically suspected to be meningiomas and one superficial glioblastoma.
Results: Patients' ages ranged from 59 to 80 years. MRIs showed extra-axial dural-based masses with contiguous but not primary brain involvement. The histopathologic and immunohistochemical diagnoses are tabulated. All primary sites were confirmed by subsequent clinical and radiologic evaluation except one case with immunoprofile for colorectal cancer where workup has yet to reveal a primary tumor.

Features of Dural-Based Metastases

Age/Sex	Location	Radiology Impression	Immunoprofile	Path Proposed Primary	Confirmed Primary	Mode of Primary Confirmation
78/M	Frontal, temporal, & parietal	Multiple meningiomatosis	CK20+, PSA+, CK7-	Prostate	Prostate	Chart review; Previous outside diagnosis
75/M	L parietal	Meningioma	Pankeratin+, PSA+, CK7-, CK20-, TTF1-, CDX2-	Prostate	Prostate	CT showing enlarged prostate & bladder invasion
59/F	L frontal	Meningioma or metastasis	Pankeratin+, CK7+, CK20-, TTF1-, CDX2-, ER-, PR-	Breast	Breast	Subsequent breast biopsy showing invasive ductal carcinoma
80/M	R parieto-occipital	Meningioma	Pankeratin+, CK7+, TTF1+, chromogranin+, CK20-, CDX2-	Lung	Lung	CT showing lung mass with hepatic & adrenal metastases
71/F	L frontal	Meningioma or metastasis	CK20+, CK19+, CDX2+, CK7-, TTF1-	Colorectal	?	N/A
59/M	R parietal	GBM involving dura	CK7+, CK19+, CK20-, TTF1-, CDX2-, PSA-	Lung, upper GI, pancreatico-biliary, or head & neck	Lung	PET showing lung mass

Conclusions: It is important for Neurosurgeons and Neuropathologists to be aware that carcinomas of diverse primary sites, including prostate, can present with dural-based masses radiologically mimicking meningiomas; therefore the surgery type can be suitably modified based on frozen section diagnosis. Moreover, a judicious combination of a screening immunohistochemical panel in conjunction with relatively specific transcription factors and hormone receptors can determine the primary tumor site with reasonable precision and guide oncologic therapy.

1695 Intratumoral Heterogeneity of Chromosomal 1p/19q Status among Glial Neoplasms: Correlation with Outcome

N Schiavo, M Brunelli, G Martignoni, F Menestrina, F Lupidi, C Ghimenton. University of Verona, Verona, Italy; Ospedale Civile Maggiore, Verona, Italy.
Background: Loss of 1p/19q is considered an important diagnostic and favourable prognostic parameter in oligodendrogliomas. Fluorescent in situ hybridization (FISH) is one of the most used technique for investigation of 1p/19q status in paraffin-embedded tissues. Heterogeneous intratumoral pattern of fluorescent signal scoring have been sometimes reported. We sought to assess different pattern and heterogeneity of 1p and 19q status among glial neoplasms.
Design: To test 1p/19q regions FISH analysis was used in a series of 49 glial neoplasms (26 oligodendrogliomas, 16 astrocytomas, 7 oligoastrocytomas) and 5 gliotic brain tissue as controls. For each case at least 200 nuclei were scored for fluorescent signals and different cut-offs were calculated to distinguish different pattern. We reported survivals on 32 patients among a period of 8 years (range: 3-8 years).
Results: 69% of oligodendrogliomas showed both chromosome 1p/19q deletions, 12% were not deleted, 12% presented gains of 1p signals, 8% displayed a polysomic pattern. Among cases with 1p/19q deletions, 12 cases (46%) showed heterogeneous population of nuclei characterized by gains and loss at 1p associated with deletion of 19q. Astrocytomas showed deletions of chromosomes 1p/19q in 6% of cases, polysomy in 81% whereas 7% were not deleted. Three oligoastrocytomas presented deletion, three with polysomy and one with gains of 1p Survival rate at the 8th year of observation was better in oligodendrogliomas (60%) than in astrocytomas (20%). Survival analysis revealed a similar trend between oligodendrogliomas with 1p/19q deleted pattern and tumours having heterogeneous pattern (about 70% of patient of both groups were alive at 8th year from diagnosis).
Conclusions: 1p/19q loss is more frequent in oligodendroglioma than in astrocytoma, the latter characterized by a polysomic pattern. Oligodendrogliomas present subgroups, such as isolated gains or heterogeneous gains and loss of 1p associated to loss of 19q, that could be referred as having a deleted pattern with a similar time of overall survival. 1p/19q status in oligoastrocytomas probably reflects the more oligodendrocytic or astrocytic nature of the neoplasm.

1696 Immunohistochemical Expression of WT1 in Gliomas

N Schiavo, G Martignoni, M Brunelli, F Menestrina, F Lupidi, C Dell'Agnola, T Sava, M Frizziero, C Ghimenton. University of Verona, Verona, Italy; Ospedale Civile Maggiore, Verona, Italy.
Background: WT1 was initially described as a tumour suppressor gene associated with nephroblastoma and interaction of this molecule with p53, Bcl-2, IGF1R, CMYC genes have been described with oncogenic-oncosuppressor effects. WT1 target therapies have been proposed in various type of neoplasms and its inhibition on glioblastoma culture cells determines regression of proliferation.WT1 immunoexpression is observed in

neoplastic astrocytes and correlates with grading of gliomas. Little is known among WT1 immunoexpression in oligodendroglial neoplasms.
Design: 83 glial neoplasms (30 oligodendrogliomas,13 astrocytomas, 8 oligoastrocytomas, 32 glioblastomas) fixed in FineFIX-paraffine embedded have been tested with Monoclonal WT1, Clone 6F-H2. Glioblastomas included also 7 glioblastoma with oligodendroglioma component, 2 gliosarcomas, 3 small cell glioblastomas and 6 giant cell glioblastomas. Scoring immunoexpression was evaluated as follows: 1+= 0-30%; 2+= 31-60%; 3+= 61-100%.
Results: 88% of glioblastomas, 70% of grade III astrocytomas showed score 3+. Gliosarcomas presented a lower expression in the sarcomatous component (less than 10% of positivity). 100% of low grade and 68% of high grade oligodendroglioma and 87% of oligoastrocytomas scored 1+. Aforementioned WT1 positive immunoexpression is observed in the cytoplasms. Gemistiocytes, minigemistiocytes, perivascular, perinecrotic and subpial neoplastic astrocytes display strong immunoexpression.

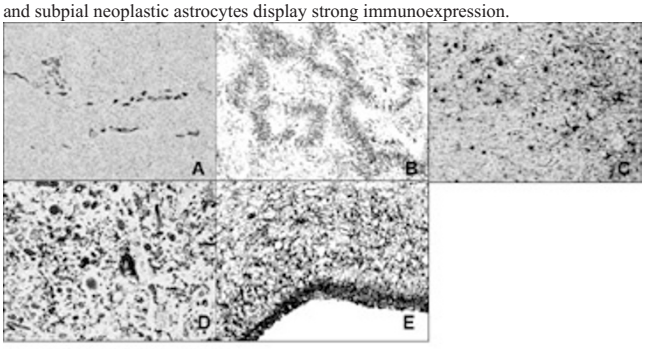

Conclusions: WT1 is a useful diagnostic marker to distinguish astrocytic and oligodendroglial tumors. WT1 immunoexpression correlates with grading of the neoplasm among astrocytic neoplasms (astrocytomas and glioblastoma). WT1 helps to evaluate astrocyitic component in oligoastrocytomas respect to oligodendroglial proliferation.

1697 Metastasis Infiltration: An Investigation of the Post-Operative Brain-Tumor Interface

MJ Schniederjan, B Raore, DJ Brat, HK Shu, JJ Olson. Emory University School of Medicine, Atlanta, GA.
Background: After surgical resection of metastatic brain tumors, stereotactic radiosurgery (SRS) is targeted at the resection cavity and surrounding tissue in order to treat potential residual invading tumor cells. The treatment area, or clinical target volume (CTV), includes normal tissue surrounding the surgical cavity. To date, no systematic investigation of the amounts of tumor cells in tissue surrounding resection cavities has been conducted. We biopsied surrounding tissue after gross total resection to evaluate the biological basis for treating with SRS beyond the cavity margin.
Design: Eleven surgical cavities were examined in ten patients. Intra-operatively after gross total resection, multiple needle-core biopsies of the margins were taken and oriented relative to the tumor (proximal-distal) to assess the amount and extent of peritumoral infiltration by residual cells. These biopsies were examined histologically and the findings recorded.
Results: Microscopic examination of multiple levels of each biopsy failed to disclose even a single residual tumor cell in any case. The only abnormal finding in the biopsies was reactive gliosis, mostly limited to the proximal/tumor end of the tissue.
Conclusions: Lack of evidence of metastatic tumor cell infiltration into surrounding brain may suggest the need to only target the resection cavity margins or gross tumor volume, in the case of metastatic solid tumors, in order to prevent treatment size dependent SRS complications.

1698 Pediatric Oligodendrogliomas: Is 1p 19q Deletion More Common Than Previously Thought?

MJ Schniederjan, AJ Janss, C Mazewski, DJ Brat. Emory University School of Medicine, Atlanta, GA.
Background: Although common among adult primary brain tumors, oligodendrogliomas (ODG) are rare in pediatric patients and little is known about how they compare with thier adult counterparts. Deletion of chromosome arms 1p and 19q is common in adult ODG and predicts a better prognosis, especially in anaplastic cases. However, in previously published series of pediatric ODGs, only three of 36 patients showed deletion of 1p & 19q, all in patients older than 10 years. Here we examine the clinicopathologic findings and 1p/19q status in a consecutive series of pediatric ODG at our institution.
Design: The surgical pathology archive at the authors' institution was searched for cases of ODG occuring in patients 18 years or younger between the years 2000 and 2009. Ten cases were found and reviewed for diagnosis and clinical and radiologic information. Fluorescence in-situ hybridization (FISH) for loci at 1p36 and 19q13 was performed in eight cases, but material for two cases was unavailable for FISH at the time of submission.
Results: Males outnumbered females (7:3) and the mean age at diagnosis was 10.6 years. Four lesions arose in the temporal lobe, two in the thalamus, two in the parietal lobe, and one in the frontal lobe. The most common presenting symptom was seizures, followed by headache. The histologic appearance in each case was diagnostic for ODG. All cases except one were WHO grade II. MIB1 positivity ranged from 1 to 10% in grade II lesions, and was 15% in the sole grade III case. FISH showed half of the tested tumors to be 1p & 19q co-deleted (4/8), 2 of which were in the first decade of life.
Conclusions: The results of 1p/19q analysis in this study are in contrast to those of previous studies, with half of tested cases showing co-deletion, whereas other patient characteristics, such as male predominance and mean age of presentation, are similar. This series is the first showing a significant percentage of co-deleted pediatric ODG. The presence of 1p 19q co-deletion suggests that pediatric oligodendrogliomas may be more genetically similar to the adult variety than previously observed.

1699 Papillary Glioneuronal Tumors — Clinicopathological and Ultrastructural Studies

JH Seo, BM Kim, JK Myung, CK Park, SH Park. Seoul National University Hospital, Seoul, Republic of Korea.
Background: Papillary glioneuronal tumor (PGNT) is an uncommon and morphologically distinct glioneuronal tumor originally described by Komori et al. in 1998. [2]. It is characterized by a biphasic pattern of pseudopapillary structures and solid sheets of monotonous cells with an often myxoid background.
Design: Clinicopathological analyses of 4 recent cases of PGNT were conducted, including immunohistochemical and ultrastructural examination and assessment of biological behavior.
Results: The patients ranged in age from 12 to 75 years (mean age: 28.4 years), had a male to female ratio of 3:1, and presented with seizures (n = 3) or muscle spasms (n = 1). The tumor location was supratentorial [frontal lobe (n = 3) and parietotemporal lobe (n = 1)]. Radiologically, they were large cystic mass with an enhancing cyst wall and mural nodules. There were 2 cases of atypical grade and 2 cases of low grade PGNTs (WHO grade I). The two atypical cases showed a high mitotic rate (4–7/10 HPF), and vascular endothelial hyperplasia and necrosis. The tumor cells were immunolabelled for glial and neuronal markers. Ultrastructural analysis revealed that these neoplastic cells exhibited characteristics of either astrocytic or neuronal differentiation, such as glial-type intermediate filaments, microtubules, and synapses with synaptic junctions and synaptic vesicles. Our patients were symptom- and progression-free, without tumor recurrence, for up to 12 to 26 months after gross total resection.
Conclusions: These cases led us to conclude that PGNT is unique among the glioneuronally-differentiated tumors, and most probably arises from neural progenitor cells. The follow-up duration of the present study was not sufficiently long to determine the biological behavior of the PGNTs, which were considered WHO grade I, but could have been of a higher grade.

1700 pHH3: Useful Marker for Evaluating Mitotic Activity in Astrocytic and Meningeal Tumors

JH Seo, JK Myung, SH Park. Seoul National University Hospital, Seoul, Republic of Korea.
Background: Mitotic count is the important criteria for grading and prognosis of most of CNS tumors. Immunohistochemical staining (IHC) for anti-phospho-histone H3 (pHH3), is previously reported that determines mitotic activity rapidly and separates mitotic figures from apoptotic nuclei easily and objectively. Therefore we compared the result of the mitotic count using anti-pHH3 IHC, conventional mitotic count on H&E slide and the Ki-67 labeling index and investigated any nonspecific staining of pHH3 in various grades of astrocytic and meningothelial tumors.
Design: Total 125 cases including 44 astrocytic tumors and 81 meningothelial tumors were investigated. For determining mitotic activity, the highest mitotic count per 10 HPF and the Ki-67 labeling index were determined. For pHH3, number of positive nuclei per 10 HPF was counted, and when the labeled nuclei were not clearly identified as mitotic figures, pHH3 labeling index was calculated with the same method for Ki-67.
Results: pHH3 was specifically positive in mitotic nuclei in astrocytic tumors but in meninigioma, nonspecific positive nuclei were found despite of extremely high dilution of pHH3 from 1:10,000 to 1:200,000. In 75.2% (81.8% of astrocytic tumors and 71.6% of meningothelial tumors) of studied tumors, the number of pHH3 positive mitoses is higher than conventional mitotic counting. In astrocytic tumors, pHH3-positive nuclei per 10HPF was well correlated with both Ki-67 labeling indices (correlation coefficient= 0.6 $p<0.001$) and WHO-grade of tumors (correlation coefficient=0.57 $p=0.001$). In meningiothelial tumors, the number of pHH3-postivie mitoses per 10HPF was well correlated with WHO-grade of tumors (correlation coefficient=0.76, $p<0.001$). However, pHH3 labeling indices, which include non-mitotic nuclei was well correlated with mitotic activity (correlation coefficient=0.55, $p=0.02$) and Ki-67 labeling indices (correlation coefficient=0.60, $p=0.001$), but not with WHO-grade of tumors.
Conclusions: pHH3 immunostaining was helpful for evaluating the mitotic activity of astrocytic tumors, but in meningiomas, it was not helpful because of nonspecific staining. Since pHH3 was more sensitive to detect mitoses than conventional counting on routine H&E slides, the criteria of mitoses for the grading of astrocytic and menigeal tumors should be shifted, otherwise we have to change the grade of the tumor after counting of mitoses on pHH3 immunostaining.

1701 Smear Analysis in the Intraoperative Diagnosis and Grading of Diffuse Gliomas: Value and Management Implications

S Sharma, R Kolhe, C Alleyne, M Reid-Nicholson. Medical College of Georgia, Augusta, GA.
Background: This retrospective cytologic study examines the value and limitations of intraoperative smears in diffuse gliomas.
Design: A retrospective review of the pathology files yielded intraoperative smears from 33 gliomas of astrocytic and oligodendroglial lineage. All cytology smears were blindly reviewed and classified by 2 pathologists, one neuropathologist and the other cytopathologist using the following criteria: cellularity, fibrillary background,

vascularity, vascular hyperplasia, nuclear shape, nuclear chromatin, pleomorphism, necrosis, mitosis, apoptosis, and Rosenthal fibers.

Results: There was concordance between smear and final neuropathologic diagnosis regarding both lineage and grade by WHO classification in 25/33 (75%) diffuse gliomas, and the closely mimicking pilocytic astrocytomas (PA). When compared with the final neuropathologic diagnosis, six glioblastoma, 5/10 anaplastic astrocytomas (AA), and one anaplastic oligoastrocytoma (AOA) were correctly classified and graded. Of grade II tumors, 5 astrocytomas (A), 3/4 oligodendrogliomas (O), 2 oligoastrocytomas (OA), and 4/5 PA, including one high-grade were correctly classified. Discrepant cases are described in Tables I and II.

Table I: Gliomas showing discrepancy in WHO grade

Cases	Smear Diagnosis	Final neuropathologic Diagnosis	Discrepancy	Technical reason	Interpretational reason
1	A (grade II)	PA	Minor	1.Thick smear 2. Sampling – absence of Rosenthal fibers	
2	A (grade II)	AA (grade III)	Major	1. Sampling 2. Sparse cellularity	
3	A (grade II)	AA (grade III)	Major	1. Sampling 2. Sparse cellularity	
4	AA (grade III)	PA	Major	1.Thick smears 2. Blood and eosin stain deposits	1. Cellularity, atypia and smudgy chromatin of protoplasmic astrocytes 2. Vascular hyperplasia; in PA.

Table II: Gliomas showing discrepancy in lineage classification

Cases	Smear diagnosis	Final neuropathologic diagnosis	Discrepancy	Technical reasons	Interpretational reasons
1	OA	O	Minor	Smear-induced cell spindling	Deletion of 1p, 19q by FISH
2	AO	AA	Major	Scant tumor	Small cell astrocytoma; 30% p53+; no FISH
3	AOA	AA	Minor		90% p53+; Retained 1p, 19q
4	AOA	AA	Minor		50% p53+; Retained 1p, 19q

Conclusions: There was a high concordance between smear and final neuropathologic diagnosis in diffuse gliomas. Smear analysis is not only complementary to frozen section in the immediate surgical management of gliomas, but is also a reasonable stand-alone diagnostic test, given correct understanding of its capability and limitations.

1702 Pediatric Infratentorial Glioblastomas with Distinct Genotype on FFPE Based aCGH

S Sharma, A Free, Y Mei, SC Peiper, Z Wang, J Cowell. Medical College of Georgia, Augusta, GA; Jefferson Medical College, Philadelphia, PA.

Background: Glioblastomas (GBM) are rare in children, but reportedly have more varied outcome and suggested differences in tumor biology as compared to typical GBM of adults. We performed high resolution array Comparative Genomic Hybridization (aCGH) aiming to identify genomic copy number changes that might define pediatric infratentorial glioblastoma.

Design: Three pediatric infratentorial GBM, ages 3.5, 7 and 14 years were identified from pathology records. DNA was extracted from formalin-fixed, paraffin embedded (FFPE) samples, using the WaxFree sample isolation kit (TrimGen), labeled with biotin and hybridized to the Affymetrix 250K Sty 1 Mapping array. Call rate of >75%, for SNPs permitted optimal visualization of chromosome events using Partek Genomics Suite software.

Results: Two tumors occurred in the brainstem and one in spinal cord. While histologically typical, one brainstem tumor showed mainly pleomorphic astrocytic cells, whereas the other brainstem and spinal tumors showed a GFAP positive small cell component. Whole chromosomal gains (#1, # 2) and loss (#20) were seen only in the pleomorphic brainstem GBM, which also showed a high level of segmental genomic copy number changes. Segmental loss involving chromosome 8 was seen in all three tumors (Chr8;133039446-136869494, Chr8;pter-3581577, Chr8;pter-30480019 respectively), whereas loss involving chromosome 16 was seen in only 2 cases with small cell components (Chr16;31827239-qter, Chr16;pter-29754532). Segmental gain of chromosome 7 was shared only between 2 brainstem cases (Chr7;17187166-qter, Chr7;69824947-qter). The spinal GBM showed a relatively stable karyotype with a unique loss of Chr19;32848902-qter. None of the frequent losses, gains and amplifications known to occur in adult GBM were identified.

Conclusions: This FFPE based, high resolution DNA copy number profiling in the examined subset of pediatric infratentorial glioblastomas shows a molecular karyotype that was more characteristic of pediatric embryonal tumors rather than adult GBM.

1703 Differential Expression of STAT-6 and Activated STAT-6 in Primary Central Nervous System Lymphoma and Peripheral Diffuse Large B-Cell Lymphoma

NT Sherwood, JF Silverman, C Pu, K Ru. Allegheny General Hospital, Pittsburgh, PA.

Background: STAT-6 is a protein transcription factor and member of the signal transduction and activator of transcription (STAT) family. These cytoplasmic proteins become phosphorylated and activated by Janus kinase in response to extracellular cytokines. The phosphorylated STAT protein is then transported to the nucleus where it exerts activation of transcription. STAT6 overexpression has been reported in central nervous system (CNS) B-cell lymphoma by DNA microarray studies. Our aim was to explore the expression level of STAT6 and activated STAT6 (pSTAT6) by immunohistochemical studies in CNS B-cell lymphoma and compared to peripheral diffuse large B-cell lymphoma (DLBCL) and investigate STAT6 activation in the tumorigenesis of these two types of lymphomas.

Design: Paraffin embedded surgical specimens including 14 cases of peripheral DLBCL and 8 cases of primary CNS B-cell lymphoma were retrieved from our files. All cases were stained with STAT6 and pSTAT6. The slides were then reviewed, and staining patterns were recorded as negative, partially positive (weak or focal staining), and strongly positive.

Results: Strongly positive staining for both STAT6 and pSTAT6 were seen in 8 of 8 cases (100%) of primary CNS B-cell lymphoma. As expected, staining was cytoplasmic for STAT6 and nuclear for pSTAT6. Only 3 of 14 cases (21%) of DLBCL were strongly and diffusely positive for either stain. There was weak, focal, or partial staining for STAT6 in 2 of 14 (14%) cases and also for pSTAT6 in 6 of 14 (43%) cases of DLBCL.

Conclusions: The STAT6 and pSTAT6 markers were highly sensitive for detecting primary CNS B-cell lymphoma. The staining patterns were strongly and diffusely positive in all cases of primary CNS B-cell lymphoma. Only 3 of 14 cases of DLBCL exhibited this pattern. The remaining cases of DLBCL were either completely negative or exhibited focal, weak, or partial-positive staining. Median survival for DLBCL may be as high as 5 years depending on subtype, whereas the median survival for primary CNS B-cell lymphoma may be as low as 12-18 months. This may reflect differences in their respective tumorigenesis and related to the STAT6 activation pathway. It would be worthwhile to further investigate this phenomenon with a longitudinal study comparing survival in cases of DLBCL that are strongly positive for STAT6 versus those that are negative or only partially positive. Additionally, STAT6 and pSTAT6 may have a role in future targeted therapy for aggressive CNS B-cell.

1704 Expression of Phospho-p38 MAPK and Phospho-p44/42 MAPK in Gliomas and Correlation with Patients' Outcome

V Zolota, Z Kefalopoulou, C Sirinian, A Argyriou, H Kalofonos. University of Patras Medical School, Patras, Greece.

Background: Gliomas are devastating and aggressive human tumors and molecular pathogenesis has been under intense investigation as a part of the effort to develop more effective therapeutic strategies for these tumors. Mitogen-activated protein kinases (MAPK) are widely expressed serine-threonine kinases mediating important regulatory signals in the cell. Activation of MAPK cascades is believed to play a critical role in malignant transformation. This study investigates the role of expression of phospho-p38 and phospho-p44/42 (Erk1/2), two key components of the MAPK signalling pathway, as prognostic indicators in gliomas.

Design: The expression of p-p38 MAPK and p-p44/42 MAPK was evaluated in 62 gliomas using immunohistochemistry on formalin-fixed paraffin-embedded tissue specimens. Grade II astrocytomas were recorded as low-grade gliomas (n = 13, mean age = 47.6 ± 15.5 years, mean overall survival = 46.3 ± 12.1 months). Grade III anaplastic astrocytomas and grade IV glioblastomas were recorded as high-grade gliomas (n=49, mean age = 58.1 ± 12.3 years, mean overall survival = 18.9 ± 14.2 months). Results were expressed as %tumor cells displaying positive nuclear stain.

Results: The table lists the results. Expression of both markers was associated with more aggressive histological features (increased cellularity, nuclear atypia, mitotic activity, gemistocytes). Statistical analysis revealed a) a higher expression of both p-p38 and p-p44/42 in high-grade compared to low-grade gliomas ($p<0.001$) and b) a strong correlation between the two markers ($r = 0.689$, $p < 0.001$). Univariate analysis revealed that p-p44/42 expression was correlated with worse overall survival ($p = 0.007$). However, Cox regression failed to confirm that p-p44/42 constitutes an independent adverse prognostic factor.

Expression levels of p-p38 and p-44/42 in low- and high-grade gliomas.

	Total cases (n=62)	Low-grade (n=13)	High-grade (n=49)
p-p38	32.2 ± 20.9	9.6 ± 7.4[a]	38.2 ± 19.1[a]
p-p44/42	39.2 ± 22.7	19.4 ± 10.5[b]	44.5 ± 22.2[b]
[a, b] < 0.001			

Conclusions: Up-regulation of p-p38 and p-p44/42 in high-grade gliomas suggests that activation of MAPK signalling pathway may contribute to the acquisition of malignant properties and tumor progression in gliomas. The pathophysiological mechanism underlying the distinctive role of MAPK family in malignant transformation in gliomas as well as any putative therapeutic applications should be further investigated.

Ophthalmic

1705 Eye Pathology in Nephrogenic Systemic Fibrosis

JL Abraham, AE Barker-Griffith. SUNY Upstate Medical University, Syracuse, NY.

Background: Nephrogenic Systemic Fibrosis, first described in 2000, is a debilitating cutaneous and systemic fibrosing disorder. The two known associations with NSF include renal dysfunction and exposure to gadolinium-containing contrast agents (GCCA). Ophthalmic interest stems from the appearance of "scleral injection" in all cases reported by Levine et al and scleral plaques seen clinically in young persons with NSF.

Design: We have reported detection by scanning electron microscopy with energy dispersive X-ray spectroscopy (SEM-EDS) of gadolinium in paraffin embedded skin biopsies of NSF tissue in over 60 cases and a few autopsy cases. Only recently have two autopsy cases included the eyes. These are studied by (SEM-EDS) for evidence of gadolinium and scleral plaques.

Results: SEM-EDS show the scleral plaques to be composed entirely of calcium phosphate with no detectable gadolinium in any of these areas. Gadolinium was discovered around and in blood vessels of the choriocapillaris. In addition, the light microscopy of the scleral plaques are very different from the usual Cogan's plaques of aging.